Nanogap Array Fabrication Using Doubly Clamped Freestanding Silicon Nanowires and Angle Evaporations

Han Young Yu, Chil Seong Ah, In-Bok Baek, Ansoon Kim, Jong-Heon Yang, Chang-Guen Ahn, Chan Woo Park, and Byung Hoon Kim

We present a simple semiconductor process to fabricate nanogap arrays for application in molecular electronics and nano-bio electronics using a combination of freestanding silicon nanowires and angle evaporation. The gap distance is modulated using the height of the silicon dioxide, the width of the Si nanowires, and the evaporation angle. In addition, we fabricate and apply the nanogap arrays in single-electron transistors using DNA-linked Au nanoparticles for the detection of DNA hybridization.

Keywords: Nanogap, freestanding nanowires, angle evaporation.

I. Introduction

To characterize the intrinsic properties of molecules and DNA-mediated bio-molecules, which are of great importance to the areas of biology and medicine [1]-[4], the physical distance of a nanogap has to achieve a comparable size. In addition, if a nanogap device is to be used for DNA sensors and molecular electronics, investigation into the compatibility of the device in modern semiconductor technology as well as the possibility for chip fabrication using conventional semiconductor processes should first be carried out. In previous reports, a variety of techniques for narrow nanogap fabrication have been demonstrated: electron beam lithography [5], [6], electromigration [7], mechanical break junction [8], sacrificial layer-assisted silicon and gold nanogaps [9], and surface-catalyzed chemical deposition [10]. However, except for electron beam lithography and sacrificial layer-assisted nanogaps, all other techniques have several problems in nanogap commercialization because of the complex steps and difficulties in fabricating reproducible nanogaps and their compatibility with other semiconductor circuits and processes. Therefore, new approaches and integration [11] methods for fabricating nanogap arrays need to be developed in order to overcome these problems.

We report on the fabrication of nanogap arrays using well-known semiconductor processes and the detection of DNA hybridization using Au nanoparticle (NP) mediated DNA linkers. Nanogap arrays with various gap sizes were formed using the angle evaporation of gold and silicon shadow masks fabricated using conventional silicon etching processes. The size of a nanogap is defined by the height of silicon dioxide, the width of the suspended silicon bar, and the evaporation angle.

Manuscript received Jan. 16, 2009; revised Apr. 8, 2009; accepted Apr. 20, 2009.

Han Young Yu (phone: +82 42 860 5905, email: uhan0@etri.re.kr) and Byung Hoon Kim (email: phooby@etri.re.kr) are with Convergence Components and Materials Research Laboratory, ETRI, Daejeon, Rep. of Korea.

Chil Seong Ah (email: acs@etri.re.kr), In-Bok Baek (email: ibbaek@etri.re.kr), Ansoon Kim (email: sooni88@etri.re.kr), Jong-Heon Yang (email: delmo@etri.re.kr), Chang-Guen Ahn (email: cgahn@etri.re.kr), and Chan Woo Park (email: chanwoo@etri.re.kr) are with IT Convergence Technology Research Laboratory, ETRI, Daejeon, Rep. of Korea.

doi:10.4218/etrij.09.0109.0006

The number of nanogaps depends on the length of the freestanding silicon nanowires and the pitch between the lines exposed by electron beam lithography. The hybridizations of DNA were monitored by time-dependent trans-conductance through a nanogap. The fabricated device shows a single electron transistor featuring a AU NP as a quantum dot and hybridized DNA as a tunneling barrier due to its high resistance.

II. Methods and Materials

1. Fabrication of Nanogap Arrays

Nanogap arrays were fabricated using freestanding silicon nanowires as shadow masks and a subsequent angle evaporation of gold. To form a 3-dimensional freestanding silicon nanowire, we adopted selective Si etching and isotropic silicon dioxide etching. Dry etching of the top silicon layer to define the nanowire patterns was performed using the etch mask of an e-beam resist, and a buffered HF solution was used to achieve the freestanding nanowires by the etching of silicon dioxide. Figure 1 shows the sequential process of the nanogap formation:

(a) A negative SAL-601 e-beam resist was spun at a speed of 4000 rpm for 30 seconds on a silicon-on-insulator (SOI) chip (n-type, (100)), and the chip was baked for 1 minute at 105°C.

(b) Electron beams were exposed onto the SAL-601 using pre-designed patterns, and the exposed devices were developed for 2 minutes 30 seconds and baked at 115°C for 1 minute using a SAL-601 developer.

(c) The top silicon was etched using inductive coupled plasma (ICP) for 180 seconds with mixed reactive gases of Cl_2 and CF_4. The exposed area sustained its structure because of the protective layer of SAL-601.

(d) The SAL-601 e-beam resist was removed using a normal cleaning process and sequentially dipping the chip in acetone, methanol, and SPM (sulfuric acid/hydrogen peroxide aqueous solution).

(e) The bottom silicon dioxide layer was etched using a buffered oxide etcher (6:1) for 2 minutes. The silicon dioxide under the patterned Si nanowire was etched isotropically; thus, the etched Si nanowire appears as a freestanding structure. In this case, there is an SiO_2 hump beneath the silicon nanowire resulted from isotropic etching. The effect of the SiO_2 hump, however, is negligible because the height of the metal electrodes is nearly the same as the height of the hump.

(f) Normal e-beam lithography was conducted to define the nanopatterns onto a poly-methylmethacrylate (PMMA) positive e-beam resist.

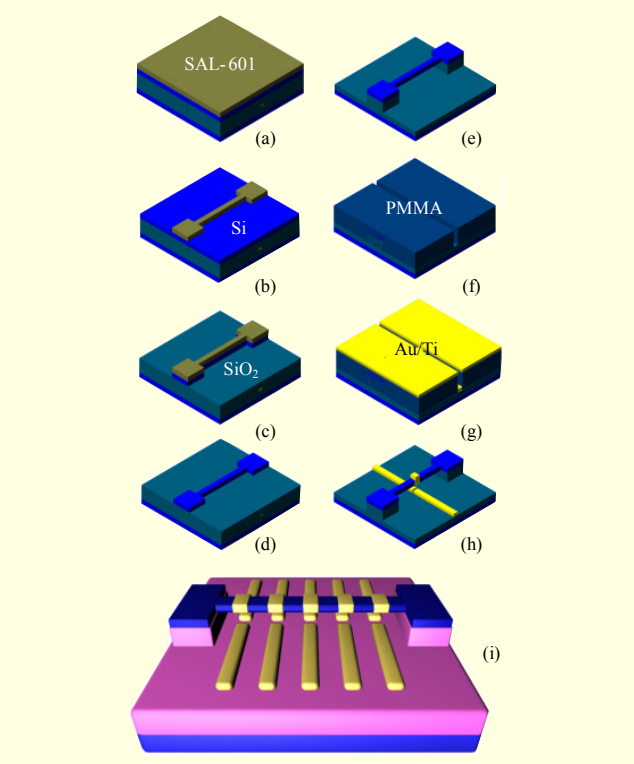

Fig. 1. (a)-(h) Fabrication process of nanogap arrays using freestanding silicon nanowire and angle evaporation and (i) a schematic diagram of nanogap arrays. We used an SOI chip with a 100 nm top silicon layer and 200 nm buried oxide.

(g) After over-developing the PMMA for 90 seconds to develop the bottom region of silicon nanowires, a Au/Ti (10 nm/5 nm) electrode (where Ti is an adhesion layer between Au and SiO_2 and Au is a substrate to thiol-terminated (-SH) DNAs) was evaporated subsequently at resolved angles.

(h) A lift-off process using acetone dipping for 2 hours followed.

Figure 2(a) shows a schematic diagram of the angle evaporation. The size of the nanogap depends on the variable dimensions such as evaporation angles (left angle θ, and right angle ϕ), the distance between the freestanding silicon nanowire and the surface of silicon dioxide (h), and the upper silicon width (w). The resulting nanogap, d, can be expressed as

$$d = w - h(\tan\theta + \tan\phi).$$

When w and h are fixed, the nanogap size relies only on the evaporation angles θ and ϕ. Suppose that angles θ and ϕ are nearly equal, then

$$d = w - 2h\tan\theta, \quad \text{if } \theta \sim \phi.$$

We set the silicon nanowire to be 100 nm wide, and the distance between the silicon nanowire and the silicon dioxide to be 180 nm. To fabricate 10 nm gold metal gaps, we first evaporated a metal adhesion layer of titanium perpendicular to

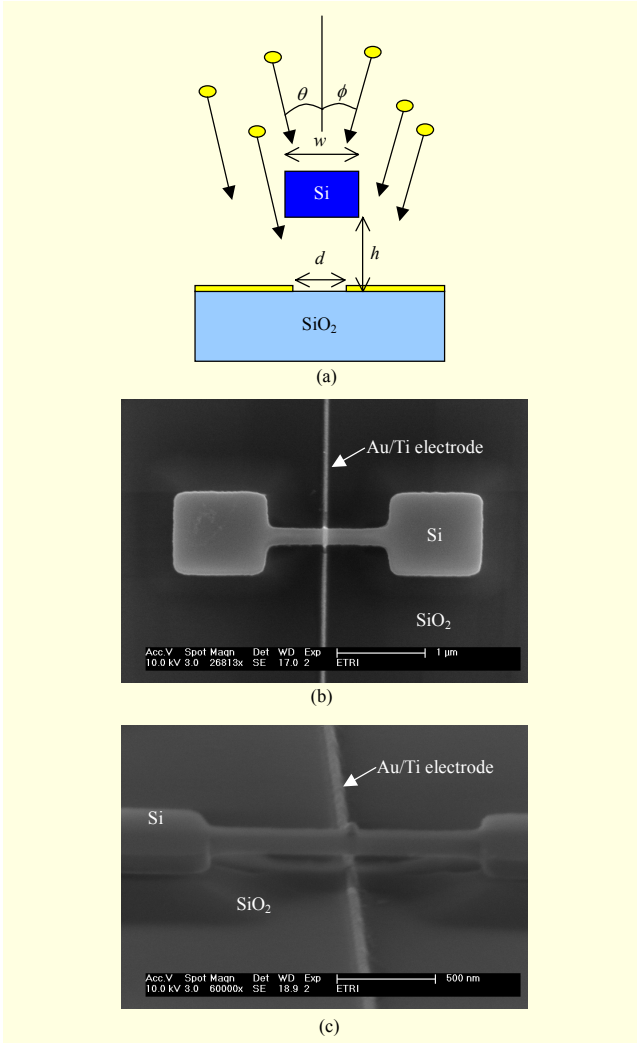

Fig. 2. (a) Schematic diagram of angle evaporation process, (b) SEM image of the top view of the nanogap and top silicon, and (c) SEM image of the side view of the nanogap and freestanding silicon nanowire.

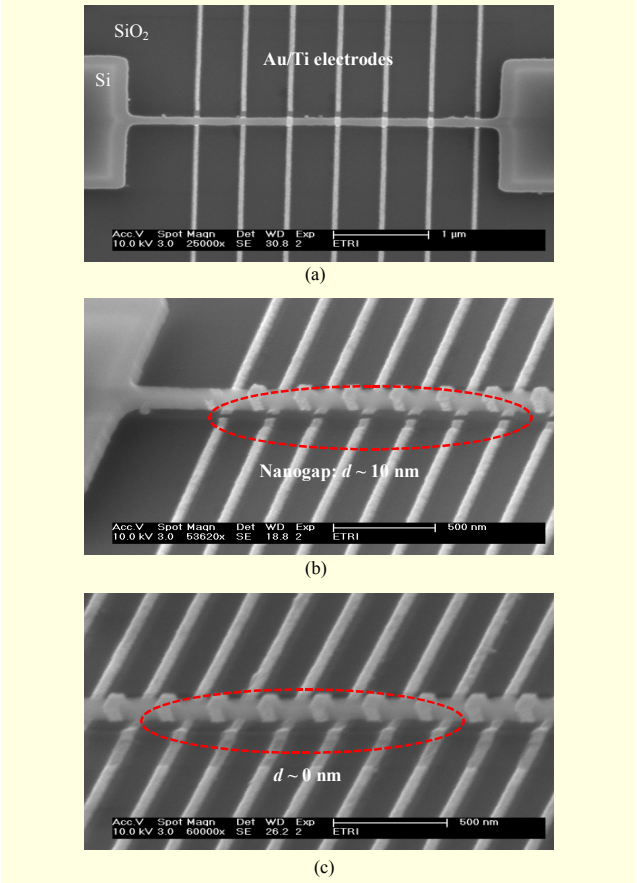

Fig. 3. SEM images of metal nanogap arrays: (a) top view, (b) side view with a freestanding silicon nanowire, and (c) side view with linked metal array.

the silicon plane and at an evaporation angle of 0°, followed by evaporation of the titanium again at an angle ($\theta \sim \phi$) of 14°. The gold evaporation followed using the same steps. In order to achieve a good precision of an evaporation angle, we used a rotation controller equipped with a stopper and gears.

As a result of the isotropic silicon dioxide etching and angle evaporations, a freestanding single silicon nanowire and resulting nanogap were achieved as shown in Figs. 2(b) and (c), which are scanning electron microscopy (SEM) images. The estimated dimension of the nanowire in the SEM images is 1 μm long, 100 nm high, and 100 nm wide. The height of the silicon dioxide beneath the silicon crystal is 180 nm measured using a profilometer and an atomic force microscope.

To fabricate the metal nanogap arrays, we exposed electron beams with multiplexed lithography on the PMMA e-beam resist, followed by metal evaporation and a lift-off process. Figure 3 shows SEM images of the fabricated nanogap arrays and the resulting metal gaps narrower than 10 nm between the Au electrodes. When the evaporation angle is higher than 14°, the gap goes to zero ($d \sim 0$ nm). The pitch between the electrodes is 250 nm and the width of the metal is lower than 100 nm. In addition, to obtain a replica nanogap array in an SOI chip, we aligned the chip parallel to a rotational axis using global marks on the chip and the axis of a sample mounter.

2. Modifications of DNA

To test the viability of applying the proposed nanogap arrays in biosensors, we used the fabricated nanogap devices for the detection of DNA hybridization between capture DNA on the Au electrodes and probe DNA conjugated with a gold NP. The gold (Au) NPs were prepared by citrate reduction of $HAuCl_4 \cdot 3H_2O$ [12] and then modified with probe DNA (5'-TCT CAA CTC GTA-SH-3') by adding the DNA into 10 mL of aqueous NP solution (particle concentration of

approximately 12 nM). The solution was then brought into a 0.1 M NaCl and 10 mM phosphate buffer (pH 7) solution, and allowed to age in this condition for an additional 20 hours. Excess reagent was removed by centrifugation for 30 minutes at 14,000 rpm. The red oily precipitate was washed twice with a 0.3 M NaCl and 10 mM phosphate buffer (pH 7) solution. After repeated purification processes, the DNA-modified NPs were finally dispersed in the 0.3 M NaCl and 10 mM phosphate buffer (pH 7) solution.

Immobilization of probe DNA-modified Au NPs into the nanogaps between electrodes was conducted as follows. First, the nanogap electrodes were coated with capture DNA by immersing the device in a solution of 5 μM capture DNA (5'-HS-CGC ATT CAG GAT-3'), 1 M NaCl, and 10 mM phosphate buffer at 50°C for 16 hours. Then, the electrodes were rinsed several times with a buffer solution containing 0.025% sodium dodecyl sulfate (SDS) in distilled water. Next, to hybridize the linker DNA (5'-TAC-GAG-TTG-AGA-ATC-CTG-AAT-GCG-3') with the capture DNA, the capture DNA-coated electrodes were immersed in 10 nM of linker DNA in a 0.3 M NaCl and 10 mM phosphate buffer (pH 7) sample solution with 0.025% SDS at 18°C for 5 hours. After the exposure to the linker DNA solution, 10 μL of a solution containing 12 nM probe DNA-modified Au NPs was dropped onto the nanogap device, and the current was then measured as a function of time between source and drain. After electrical measurement of the immobilization process of the DNA-modified gold NPs between nanogaps shown in the inset of Fig. 4(b), the electrodes were rinsed with 0.025% SDS, 0.3 M NaCl, and 10 mM phosphate buffer solution. Finally, they were rinsed with a 0.3 M volatile ammonium acetate buffer solution to remove residual salts and nonspecifically bound Au NPs.

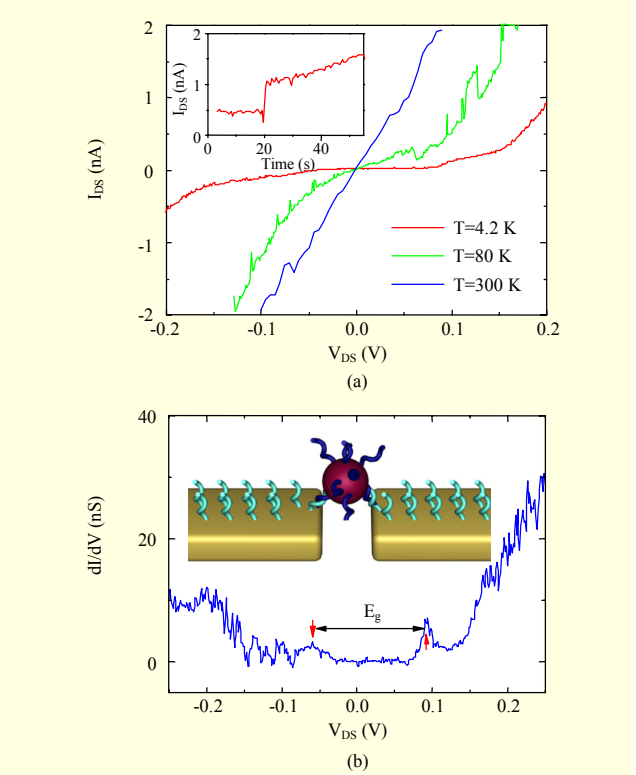

Fig. 4. (a) Current-voltage characteristics of Au NP-mediated SET at various temperatures. Current as a function of bias voltage decreases with a decrease of temperature and eventually shows a flat level (I_{DS} = 0 A) at T = 4.2 K. The inset shows pre-hybridization between the linker DNA onto a Au surface and capture DNA around the Au NPs. The inset also shows current variations as a function of time, while the injected DNA-linked Au NPs are positioned in the nanogap. (b) A differential conductance curve at T = 4.2 K. The inset shows a schematic diagram of the DNA-mediated Au NP SET.

3. Detection of DNA Hybridization

The electrical detection of DNA hybridization was performed using the current deviations as a function of time caused by the hybridization. After DNA hybridization, the open metal electrodes are electrically linked by the Au NP conjugated with target DNA, and the conductance can be expected to be increased by the quantum island of the Au NP. The change of the conductance behavior via the applied source-drain voltage, as shown in the inset of Fig. 4(a), can be used as a sensing scheme for bio-molecular detection [13]. The time-dependent current change between source and drain caused by DNA hybridization was monitored with a fixed voltage of 50 mV. The current increases abruptly at t = 20 s and is then saturated. While the device configured with the source and drain electrodes of Au metal and dielectric material of liquid solution without DNA hybridization, the reference current maintains a flattened zero level since the conducting occurs only via tunneling through the liquid medium. However, with DNA hybridization, the tunneling conductance is enhanced by the gold island between source and drain and results in an abrupt current increase as shown in the inset of Fig. 4(a).

4. Electrical Properties of DNA Linked Gold Nanoparticles

By reducing the size of a Au NP, the continuum energy state becomes discrete due to quantum confinement, and a device composed of a Au NP and hybridized DNA can be regarded as a single electron transistor [14] featuring the Au NP as a quantum dot and the DNA as a dielectric medium. Figure 4(a) shows the I-V characteristics for the Au NP quantum dot conjugated with DNA at three different temperatures, 4.2 K, 80 K, and 300 K. As the temperature decreases, the trans-conductance decreases and a Coulomb gap appears. In the

differential conductance curve obtained from the I-V characteristics at $T = 4.2$ K shown in Fig. 4 (b), conductance peaks appear which are related to the discrete energy states in the Au NP caused by quantum confinement.

The size of a Au NP quantum dot can also be estimated using the energy-level spacing in a three-dimensional sphere resulting from the quantum confinement as

$$\Delta E = (3\pi^2)^{-1/3}(\pi/6\Omega)^{-1/3}(\hbar^2\pi^2/m^*L^3),$$

where ΔE is the energy-level spacing due to the quantum confinement, Ω is the atomic volume for gold (1.69×10^{-29} m^3), $\hbar$ is the Planck constant (divided by 2π), m^* is the electron effective mass ($m^* \approx 0.08m$, m is the free electron mass) [15], and L is the diameter of the Au quantum dot. The estimated quantum dot size of the Au NP, using the level spacing $2\Delta E$ = 0.14 eV as shown in Fig. 4 (b), is 12.5 nm, which is nearly the same as the size of the Au NP (13 nm).

III. Conclusion

In summary, we have developed a technique for the fabrication of nanogap arrays for application in nano-bio sensors and mesoscopic electronic devices. By the assistance of a freestanding silicon nanowire and angle evaporation, sub-10 nm nanogaps were achieved. To verify the practical viability of the nanogap array, we applied the fabricated nanogap devices to DNA-mediated single-charge tunneling devices, where the size of the gold quantum dot calculated from the energy level spacing was well matched with the size of the gold NP as synthesized. This new technique using easy replica nanogap fabrication and semiconductor processes can be applied in molecular electronic devices.

References

[1] J. Shendure et al., "Advanced Sequencing Technologies: Methods and Goals," *Nature Reviews Genetics*, vol. 5, no. 5, 2004, pp. 335-344.

[2] E.Y. Chan, "Advances in Sequencing Technology," *Mutation Research-Fundamental and Molecular Mechanisms of Mutagenesis*, vol. 573, no. 1-2, 2005, pp. 13-40.

[3] L.J. Kricka et al., "Miniaturized Detection Technology in Molecular Diagnostics," *Expert Review of Molecular Diagnostics*, vol. 5, no. 4, July 2005, pp. 549-595.

[4] Y.S. Kim et al., "Miniaturized Electronic Nose System Based on Personal Digital Assistant," *ETRI Journal*, vol. 27, no. 5, Oct. 2005, pp. 585-594.

[5] P.B. Fischer and S.Y. Chou, "10 nm Electron Beam Lithography and Sub-50 nm Overlay Using a Modified Scanning Electron Microscope," *Appl. Phys. Lett.*, vol. 62, no. 23, 1993, pp. 2989-2991.

[6] S. Itousa et al., "Fabrication and AFM Characterization of a Co-planar Tunnel Junction with a Less Than 30 nm Interelectrode Gap," *Nanotechnology*, vol. 5, 1994, pp. 19-25.

[7] H. Park et al., "Fabrication of Metallic Electrodes with Nanometer Separation by Electromigration," *Appl. Phys. Lett.*, vol. 75, no. 2, July 1999, pp. 301-303.

[8] M.A. Reed et al., "Conductance of a Molecular Junction," *Science*, vol. 278, no. 5336, Oct. 1997, pp. 252-254.

[9] C.W. Park et al., "Fabrication of Poly-Si/Au Nano-gaps Using Atomic-Layer-Deposited Al_2O_3 as a Sacrificial Layer," *Nanotechnology*, vol. 16, 2005, pp. 361-364.

[10] C.S. Ah et al., "Fabrication of Integrated Nanogap Electrodes by Surface-Catalyzed Chemical Deposition," *Appl. Phys. Lett*, vol. 88, 2006, pp. 133116-1–113116-3.

[11] J. Kim et al., "Integration of 5-V CMOS and High-Voltage Devices for Display Drive Applications," *ETRI Journal*, vol. 20, no. 1, 1998, pp. 37-45.

[12] J. Storhoff et al., "One-Pot Colorimetric Differentiation of Polynucleotides with Single Base Imperfections Using Gold Nanoparticle Probes," *J. Am. Chem. Soc.*, vol. 120, no. 9, 1998, pp. 1959-1964.

[13] X. Liang and S.Y. Chou, "Nanogap Detector inside Nanofluidic Channel for Fast Real-Time Label-Free DNA Analysis," *Nano Letters*, vol. 8, no. 5, Apr. 2008, pp. 1472-1476.

[14] H. Grabert and M.H. Devoret, *Single Charge Tunneling*, New York: Plenum, 1992.

[15] F. Ruffino et al., "Size-Dependent Schottky Barrier Height in Self-Assembled Gold Nanoparticles," *Appl. Phys. Lett.*, vol. 89, no. 24, 2006, pp. 243113-1–243113-3.

Han Young Yu received the BS degree in physics from Yonsei University, Korea, in 1997, and the MS and PhD degrees in physics from Seoul National University, Korea, in 1999 and 2003, respectively. He has been with the Electronics and Telecommunications Research Institute (ETRI) since 2003, where he is currently a senior researcher. His research interests include biosensors, nano-electronic devices, molecular electronics, single electron transistors, and energy storage materials and systems including hydrogen storage and energy harvesting systems.

Chil Seong Ah received his BS degree in chemistry from Hanyang University, Korea, in 1996, and his MS and PhD degrees in chemistry from Seoul National University, in 1998 and 2003, respectively. He worked at the Korea Research Institute of Standards and Science as a senior researcher from March 2003 to August 2005. He has been working at Electronics and Telecommunications Research Institute (ETRI) since 2005. He is currently a senior member of engineering staff with the Biosensor Research Team at ETRI, Korea. His research interests include biosensors, surface chemistry, and synthesis of metal nanoparticles.

In-Bok Baek received the BS and MS degrees in physics from Chungbuk National University, Cheongju, Korea, in 2001 and 2003, respectively. In 2004, he joined the Electronics and Telecommunications Research Institute (ETRI), Daejeon, Korea, where he is involved in basic research on nanoscale electronic devices. From 2007 to 2008, he was involved in research on nanoelectronic biosensors. His research interests include electron beam lithography, processing and analysis of nanoscale silicon devices, single-electron devices, and logic circuit technology.

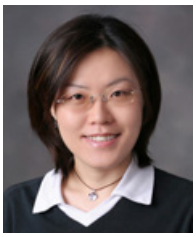

Ansoon Kim received the BS degree in chemistry from Hanyang University, Korea, in 1999, and the MS and PhD degrees in chemistry from Korea Advanced Institute of Science and Technology (KAIST), Korea, in 2001 and 2005, respectively. She is currently a senior researcher with the Electronics and Telecommunications Research Institute (ETRI). She is interested in nano-bio hybrid systems.

Jong-Heon Yang received the BS degree in electrical engineering from Korea Advanced Institute of Science and Technology (KAIST), Korea, in 2000, and the MS degree in electronic engineering from Pohang University of science and technology (POSTECH), Pohang, Korea, in 2002. He is currently a senior engineer with the Convergence Technology Research Division of the Electronics and Communications Research Institute (ETRI), Daejeon, Korea.

Chang-Geun Ahn received the MS and PhD degrees in electronic and electrical engineering from Pohang University of Science and Technology, Pohang, Korea, in 1996 and 2000, respectively. In 2003, he joined the Electronics and Telecommunications Research Institute (ETRI), Daejeon, Korea, where he has been involved in research on nanoscale silicon MOSFET devices. His current research interests include nano-devices and bio-sensors based on semiconductor device technologies.

Chan Woo Park received the BS, MS, and PhD degrees in materials science and engineering from Korea Advanced Institute of Science and Technology (KAIST), Daejeon, Korea, in 1994, 1996, and 2000, respectively. Since 2000, he has been with the Electronics and Telecommunications Research Institute (ETRI), Daejeon, Korea, as a senior member of engineering staff. His research interests include silicon-based integrated circuits, technology of micro/nanosystems, and "top-down" fabricated field effect transistor (FET)-type biosensors.

Byung Hoon Kim received the BS degree in physics from University of Incheon, Incheon, Korea in 2001, and the MS and PhD degrees in physics from Seoul National University, Seoul, Korea, in 2003 and 2007, respectively. Currently, he is a post-doctoral researcher with the Electronics and Telecommunications Research Institute (ETRI). His research interests include hydrogen storage and electrical transport properties of transition metal oxides.